The IESFOgram as a selection tool for the optimal band of integration using cyclo-non-stationary based tools in rolling element bearing diagnostics

Alexandre Mauricio[a,b], Wade A. Smith[c], Robert B. Randall[c], Jerome Antoni[d], Konstantinos Gryllias[a,b,*]

[a] *Faculty of Engineering Science, Department of Mechanical Engineering, Division PMA, KU Leuven*
Celestijnenlaan 300, Box 2420, 3001 Leuven, Belgium
[b] *Dynamics of Mechanical and Mechatronics Systems, Flanders Make, Belgium*
[c] *School of Mechanical and Manufacturing Engineering, University of New South Wales Sydney, NSW 2052, Australia*
[d] *Laboratoire Vibrations Acoustique, University of Lyon, INSA-Lyon, 69621, Villeurbanne, France*

Abstract

Demodulation methods are one of the most widely used tools for bearing diagnostics, and in particular, are methods based on the Squared Envelope Spectrum (SES) with band pass filtering. One of the main challenges of these methods is the detection of a suitable band for the demodulation of the signal under varying speed conditions. Angular resampling methods may synchronize the impulsive nature of bearing damages with a certain periodicity, in the case of large speed fluctuations. On the other hand, the time-invariant carrier frequencies may spread over the broadband of the spectrum, making impossible the application of many band selection tools. Lately, focus has been targeted to cyclostationary-based tools which show a high performance in detecting hidden cyclic periodicities in their bi-variable representation, such as the Cyclic Spectral Correlation (CSC) and the Cyclic Spectral Coherence (CSCoh). Initially, these methods have been represented in the Frequency-Frequency domain, however they have been extended to be able to describe signals under varying speed condition in the Order-Order domain and the

*Corresponding Author
Email address: konstantinos.gryllias@kuleuven.be (Konstantinos Gryllias)

Order-Frequency domain. Furthermore, the integration of these bi-variable maps on a specific band of frequencies results in equivalent to demodulated spectra which effectively exhibit the bearing cyclic frequencies, in case they are hidden under other component signatures or under the noise level. The challenge is the selection of a proper band of integration to obtain these demodulated spectra for bearing diagnostics purposes. In this paper, a novel tool called Improved Envelope Spectrum via Feature Optimization-gram (IESFOgram) is proposed as a band selection tool for the demodulation of the bi-variable map (CSC or CSCoh) for bearing diagnostics. The method is represented in a 1/3-binary tree and is applicable under constant speed conditions, using the Frequency-Frequency domain, as well as under variable speed conditions. The methodology is tested and validated on real data captured on a laboratory planetary gearbox and on an aircraft engine gearbox, under both constant and varying speed conditions. Furthermore, the methodology is also compared in terms of performance with the Fast Kurtogram and the Autogram-based methods, under constant speed operating conditions.

Keywords: Bearing diagnostics, Planetary gearbox, Speed-varying operating conditions, Cyclic Spectral Coherence, Order tracking

1. Introduction

Rolling element bearings are critical components of rotating machinery and their failure can cause sudden breakdown of the system, leading to time-loss and increased costs. Condition monitoring is the field where rotating machinery is analysed, including bearings and gears and damages that may be present on the structures can be detected. Therefore, maintenance and faulty component repair can be performed before breakdown. The diagnostics of bearings continues to be a challenge however, as their signatures are usually masked under noise and other stronger component signatures (e.g. gears). Lately condition monitoring of complex machinery has seen increased research interest, due to their wide application on critical mechanisms and to their high diagnostics difficulty caused

by the plethora of components signatures which are present. Diagnostics under varying speed conditions has also attracted increased attention in the field, as they represent the real machine operating conditions where the classical methods often fail. Typical examples, including wind turbines [1, 2], aircraft engines [3] and helicopter gearboxes [4, 5], operate usually under varying load and speed conditions, which limit the detectability of damage present on these rotating structures.

One of the most well established methods is the Envelope Analysis, where the signal is demodulated after band-pass filtering around the resonant frequencies excited by the damage impulses, obtaining in the end a filtered Squared Envelope Spectrum (SES). The main idea is to obtain an optimal filter band which presents a high Signal-to-Noise ratio (SNR) leading to a SES after demodulation where the fault harmonics are enhanced [6, 7]. The optimal selection of this frequency band for demodulation is an important, frequent and popular topic present in the field. The main reason is that some sort of filtering processing is common to most of condition monitoring applications, and the band can be selected either by engineering knowledge or by a methodology that selects the band in a (semi-)automated manner. Nowadays, the most widely used band selection tool is the Fast Kurtogram (FK) [8, 9], which is an automated band selection tool based on the maximum kurtosis level. Apart from this tool, a number of other band selection tools have been also developed to obtain the SES. Moshrefzadeh and Fasana proposed the Autogram [10], which is a tool with the same representation and the same objective of selecting the optimal band for demodulation to obtain the SES. It is also based on the maximum kurtosis, but unlike the FK, it is calculated based on the unbiased autocorrelation of the squared envelope of the demodulated signals. Moreover the Optimised Spectral Kurtosis (OSK) [11] selects the band with the maximum kurtosis as well, while retaining a narrow bandwidth in order to by-pass electro-magnetic interference noise on the signals. Additionally the Sparsogram [12] is based on the sparsity level on different bands based on the wavelet-packet, and the Infogram [13] utilizes the negentropy as a feature to detect the impulsive bands of the signal

for demodulation.

Furthermore the Cyclic Spectral Correlation (CSC) and the Cyclic Spectral Coherence (CSCoh) have been proposed in the last two decades as an alternative for the SES-based methods [14, 15, 16, 17]. The main advantage of this method falls on its ability to reveal hidden periodicities of second-order cyclostationarity, like bearing signals that are masked under stronger signals, such as the gear signals. They are represented in bi-variable maps in the frequency-frequency domain, where its spectral axis can be integrated to obtain either the Enhanced Envelope Spectrum (EES) or the Improved Envelope Spectrum (IES) [15, 18, 19]. Diagnostic features based on the sum of the gear related harmonics on the bi-variable map (CSCoh and CSC) have also been proposed, providing a good estimation of the change of conditions of planetary gearboxes [20]. Furthermore the enhancement of the CSCoh map through filtering selected by kurtosis maximization and the denoising of the CSCoh map have also been proposed in order to increase the SNR, targeting towards clear envelope spectra presenting only the fault related harmonics [21]. Thus, spectral analysis based on the bi-variable map (EES and IES) seems to improve the detection of cyclostationary faulty signals when compared to the classical SES. However, to obtain the optimal band of demodulation for the CSC or CSCoh, its bi-variable map needs to be analysed in order to select the optimal band for integration along the spectral axis. The objective of this paper is to propose a band selection tool, named the IESFOgram, which is similar to the FK but is applied on the CSC and CSCoh bi-variable maps. The IESFOgram is displayed as a color-mapped 1/3 binary tree like the FK and by the optimisation of a criterion it provides an optimal band of integration, resulting in an IES and allowing the detection of the fault frequency harmonics.

However, the abovementioned cyclostationary-based tools are based on the notion that only small speed fluctuations occur and not on the notion of varying speed conditions. Under varying speed conditions, SES-based tools are usually re-sampled in the angular domain [22], resulting in the Order Tracked Squared Envelope Spectrum (OTSES). The same Order Tracking method has also been

applied to the CSC and to the CSCoh with success, providing robust diagnosis of bearings. The methods rely on the theory that bearing faults are dependent on the shaft angle and independent of time. Therefore, the hidden periodicities remain on the angular domain although the signal are non-stationary in the time domain. This fact generated the idea of classification of the bearing signals under varying speed conditions as cyclo-non-stationary signals and as long as they are analysed on the order domain, diagnosis is possible [19, 18]. Moreover the transformation of the signals into the angular domain before the calculation of the CSC-based methods in order to obtain the Order-Order Cyclic Spectral Correlation/Coherence (OOCSC and OOCSCoh) concentrates the cyclic frequencies, resulting in a robust detection of the hidden modulations under a carrier of random frequency. On the other hand, re-sampling of the Time-Frequency domain on the angular domain, in order to obtain the Angular-Frequency domain map leading to the Order-Frequency domain of the bi-variable maps has also been proposed as a tool to detect hidden modulations for vibration analysis of rotating machinery under varying speed conditions [18, 19].

The objective of this paper is the proposal of the IESFOgram as a band selection tool to be applied on bi-variable maps based on CSC-based methods for bearings diagnostics under constant or varying speed conditions. The methodologies are validated on real signals of two datasets (one from a Safran aircraft engine gearbox and one from a UNSW planetary gearbox). Furthermore, the performance of the methodologies is compared with the band pass filtering selection based on the Fast Kurtogram and the Autogram. The rest of the paper is outlined as follows. In Section 2, the background theory needed for the application of the proposed method is detailed. In Section 3 the proposed methodology is analytically presented. In Section 4, the methodology is tested, validated and compared with state of the art methodologies under constant speed conditions, and then is further validated under varying operating speed conditions. The paper closes in Section 5 with some conclusions.

2. Background of cyclostationarity and cyclo-non-stationarity

2.1. Cyclostationary signals

Rotating mechanical components are likely to generate cyclic transient signatures which are periodic in nature if the rotational speed is kept constant during the acquisition of signals. These signals often carry information on the health of machinery components, and signal processing and feature extraction are widely used in order to extract this information and further exploit it tracking their health condition. Following the cyclostationary theory, the signals of interest acquired from rotating machinery can be defined based on the two first orders of cyclostationary signals. Signals of first order of cyclostationarity (CS1) are signals whose the first-order statistical moment is a periodic function of T complying with the condition of Eq. 1.

$$C_{1x}(t) = \mathbb{E}\{x(t)\} = C_{1x}(t+T) \tag{1}$$

where $\mathbb{E}$ denotes the ensemble averaging operator, and t stands for the time. In rotating machinery, CS1 vibrations signals are periodic waveforms related to components phase-locked with the rotor speed(*e.g.* shaft misalignment, spalling on meshing gears, etc.). On the other hand, a second-order cyclostationary (CS2) signal is a signal whose the second order statistical moment is periodic [23]. In particular, its autocorrelation function is periodic with period T as described in Eq. 2.

$$C_{2x}(t,\tau) = \mathbb{E}\{x(t)x(t-\tau)^*\} = C_{2x}(t+T,\tau) \tag{2}$$

where τ corresponds to the time-lag variable. Bearing vibration signals are often described as CS2, due to having a hidden periodicity related to the shaft speed. Finally, nth-order cyclostationary (CSn) is a signal whose the nth-order statistical moment is periodic, but generally speaking signals with higher order than CS2 are usually not taken into account, as CS1 and CS2 describe well the signals of interest generated by rotating machinery.

The Cyclic Spectral Correlation (CSC) is a tool where the CS1 and CS2 signals are well described in the frequency-frequency domain. The method is

represented as a distribution function of two frequency variables: the *cyclic frequency* α linked to the modulation and the *spectral frequency* f linked to the carrier signal. The tool can be described also as the correlation distribution of the carrier and modulation frequencies of the signatures present in the signals, defined in Eq. 3.

$$CSC(\alpha, f) = \lim_{W \to \infty} \frac{1}{W} \mathbb{E}\{\mathscr{F}_W[x(t)]\mathscr{F}_W[x(t+\tau)]^*\} \tag{3}$$

where $\mathscr{F}_W[x(t)]$ stands for the Fourier transform of the signal $x(t)$ over a finite time duration of W. Processing the CSC results in the bi-variable map, which reveals the hidden modulations, making it a robust tool for detecting the cyclostationarity in vibration signals [17, 15].

In order to minimize uneven distributions, a whitening operation can be applied to the CSC. This extended tool, named the Cyclic Spectral Coherence (CSCoh), describes the spectral correlations in normalized values between 0 and 1, and is defined as in Eq. 4:

$$CSCoh(\alpha, f) = \frac{CSC_x(\alpha, f)}{\sqrt{CSC_x(0, f)CSC_x(0, f+\alpha)}} \tag{4}$$

Both the CSC and the CSCoh bi-variable maps can be integrated along the spectral frequency axis in order to obtain a regular spectrum, resulting in a one dimension spectrum function of the cyclic frequency α. The band of spectral frequencies to be integrated can be defined as the full available band, from zero up to the Nyquist frequency, resulting in a spectrum that exhibits all modulations present in the signal. On the other hand, the band can be defined as the one that maximizes the cyclic characteristic frequency of interest while minimizing the background noise and the other frequency components that may mask the frequency of interest. In this manner, the integration over a specific band on the bi-variable map can improve the detection rate of the characteristic frequency related to the present damage on the signal. The resulting spectrum is then named Improved Envelope Spectrum (IES) and it is obtained from the frequency-frequency domain according to Eq. 5 :

$$IES(\alpha) = \frac{1}{F_2 - F_1} \int_{F_1}^{F_2} |CSCoh_x(\alpha, f)| df \tag{5}$$

2.2. Cyclo-non-stationary signals

Signals with an hidden periodicity related to the shaft angle can be defined as cyclostationary in time under constant speed operating conditions. However, under varying speed conditions, the impulses related to the shaft speed are no longer cyclostationary in time, and carriers related to time are no longer cyclostationary in angle. Thus, they are defined as non-stationary. This signal nature is known to be the definition of the signal of rolling element bearings under varying operating conditions. Although the signals are neither time nor angle-cyclostationary, a hidden periodicity is still present in the signal. These signals are classified as Cyclo-Non-Stationary (CNS) signals, and some order tracking techniques can be applied to the bi-variable map.

The signal can be resampled into constant angle intervals before the calculation of the CSC. Considering the time variable t as a function of equal intervals of angle θ and angle-lag ϕ as $t(\theta)$ and as $t(\theta + \phi)$,the CSC in the Order-Order domain can be extracted, as defined in Eq. 6.

$$OOCSC(\alpha(\theta), f(\phi)) = \lim_{W \to \infty} \frac{1}{W} \mathbb{E}\{\mathscr{F}_W[x(t(\theta))]\mathscr{F}_W[x(t(\theta + \phi))]^*\} \quad (6)$$

The method results in the bi-variable map function of spectral variable f and cyclic variable α, which are now described in units of $orders$ function of the shaft speed. Therefore, the bi-variable function can be denominated as Order-Order Cyclic Spectral Correlation (OOCSC). The Order-Order Cyclic Spectral Coherence (OOCSCoh) can be extracted just as described previously in Eq. 4, with the difference being that the variables α and f are now function of angle, and thus are represented in orders of the shaft speed.

Angle-cyclostationary signals are well represented with this method, however CNS signals with time-invariant phenomena result in a distortion along the spectral variable order axis f. In alternative, the so called "angle-time cyclostationary" (AT-CS) processes can be applied in order to extract a bi-variable function of angle in the cyclic variable axis α and function of time in the spectral variable axis f. This prevents the spread distribution of the time-invariant carrier coefficients along the spectral axis, as well as preventing

the spread distribution of the angle-invariant modulation coefficients along the cyclic axis. The process can be defined as the correlation between two time instants locked in angle position θ and spaced apart by a given time-lag τ. Therefore, the correlation function between $t(\theta)$ and $t(\theta) - \tau$ results in the CSC function in the Order-Frequency domain (OFCSC) as defined in Eq. 7.

$$OFCSC(\alpha(\theta), f(t)) = \lim_{W \to \infty} \frac{1}{W} \mathbb{E}\{\mathscr{F}_W[x(t(\theta))] \mathscr{F}_W[x(t(\theta) + \tau)]^*\} \quad (7)$$

where the cyclic variable *alpha* is a function of the angle θ, while the spectral variable f is a function of time t.

One useful definition of the CSC is as the double Fourier transform of the covariance. For the Frequency-Frequency domain, the Time-Frequency domain of the signal is extracted as a function of time, and then the second Fourier transform is applied to obtain the Frequency-Frequency domain CSC. In case the signal is tracked in the angular domain, the Short Time Fourier Transform results in the Angle-Order domain, and a further Fourier transform results in the Order-Order CSC. On the last case, the order tracking is applied on the Time-Frequency domain, resulting in the Angle-Time domain. Applying a second Fourier transform results then in the Order-Frequency CSC.

The use of these three different domains is a useful concept to take into account depending on the nature of the signal to be analysed. For example, given a simulated signal of an outer race damage on a rolling element bearing under varying speed conditions, the carrier frequency of the excited resonant frequency can be extracted at the spectral variable axis using the CSC in the Frequency-Frequency domain. However, as the cyclic impulses are angle-invariant, the impulse frequency of the fault is spread over the cyclic variable. The Order-Order domain of the CSC concentrates the cyclic modulations on the cyclic axis, but on the other hand the carrier cannot be extracted, as the carrier frequency is time-invariant and the spectral axis is represented in function of angle (orders). Lastly, the Order-Frequency domain of the CSC allows the extraction of both the carrier frequency and the cyclic order of the damaged bearing signal.

The speed profile and bi-variable maps in the three domains are presented in

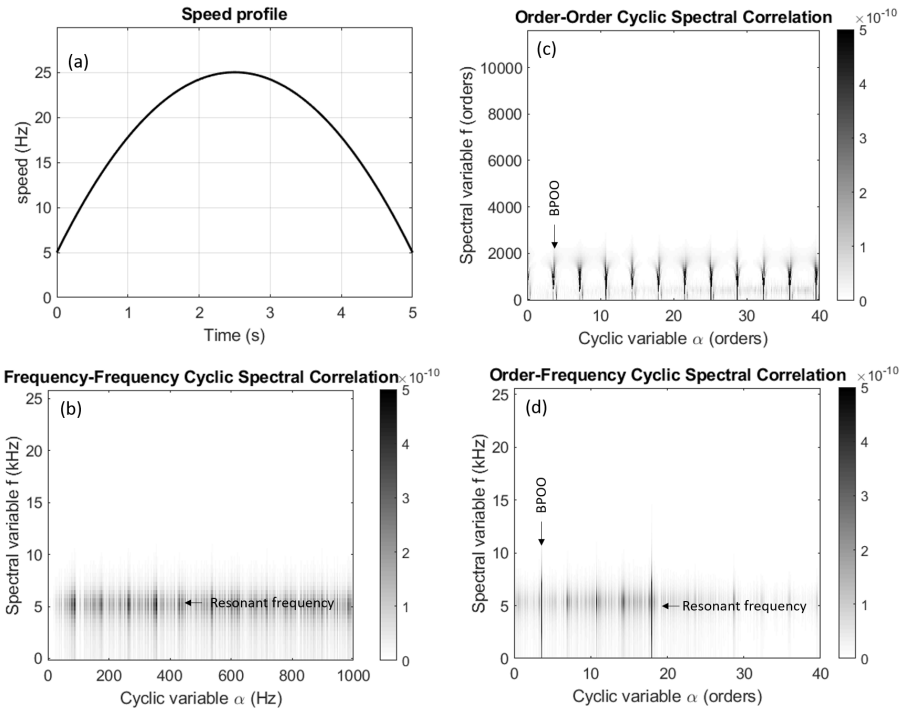

Figure 1: (a) Instantaneous speed of the signal, (b) Frequency-frequency domain CSC, (c) Order-Order CSC, (d) Order-Frequency CSC.

Fig. 1 as a demonstration of the described phenomenon. A bearing signal with a Ball Pass Order of the Outer race (BPOO) of 3.5 orders of the shaft speed, with a carrier frequency of 5 kHz, and varying speed following a parabolic function is simulated using a bearing model [24] in order to demonstrate the described phenomena in the three domains.

3. Proposed methodology

Diagnosis using the bi-variable maps require a deep understanding of the map in order to exploit its information. The analysis of one dimensional spectra is far more easy and therefore widely applied in the academia and industry. It has been seen that the integration of the bi-variable function along

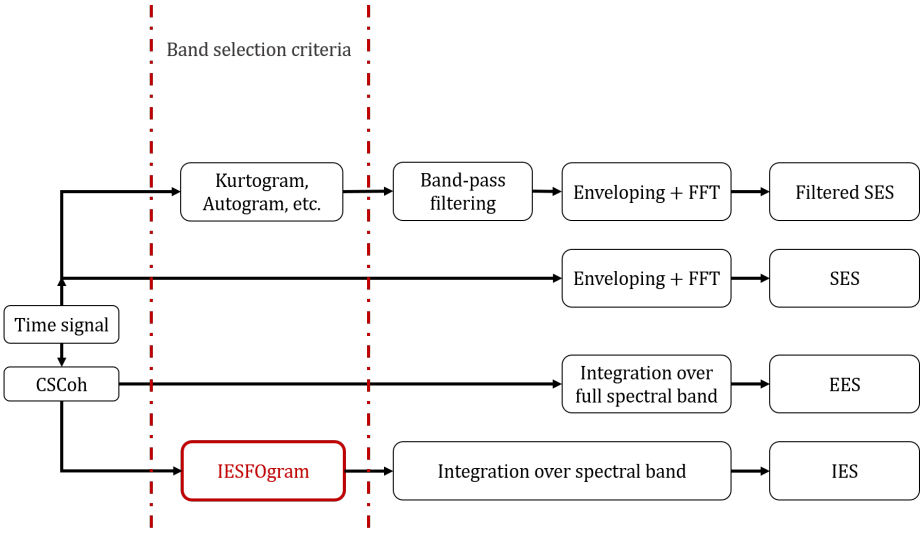

Figure 2: Schematic description of EA, classical SES, EES and IES.

its spectral variable results in a one dimensional spectrum, which would be a good tool on itself for diagnostics purposes. On the other hand, the diagnostics information could still be masked under the noise and other components signatures. Integration of the specific band that carries the signal of interest can further enhance the spectrum and increase the performance in the detection of the frequencies (or orders) of interest. The detection of the optimal band of integration on the bi-variable map is not always straightforward.

This paper proposes a band selection tool for the detection of the carriers of the cyclic modulations of interest present in the bi-variable map. Band selection tools are known to be applied in the classical methods, and the novelty of this paper is to provide a band selection tool, named Improved Envelope Spectrum via Feature Optimization-gram (IESFOgram), to be applied in the bi-variable map as placed in the scheme depicted in gray in Fig. 2.

The proposed method tries to optimize a Diagnostic Feature (DF) based on the cyclic characteristics of interest (e.g. the rolling element bearing characteristic fault frequencies/orders) on the demodulated spectrum resulting from the integration of the bi-variable map. The method is thought to be

general enough to be applied to either the CSC or the CSCoh in any of the three domains: Frequency-Frequency; Order-Order; and Order-Frequency. As such, the variables on the cyclic axis *alpha* and spectral axis f are not defined as specifically function of time or function of angle, and therefore any generic unit for the two variables may be used in the detailing of the proposed method. The resolution of the cyclic frequency α is equal to the proportional inverse of the length of the signal. In other words, the cyclic frequency resolution $\mathrm{d}\alpha$ will be equal to $1/T_d$, where T_d is the time duration. Moreover the cyclic order resolution $\mathrm{d}\alpha$ will be equal to $1/N_r$, where N_r is the number of measured shaft rotations. The resolution of the spectral frequency $\mathrm{d}f$ is equal to the half of the sampling frequency ($fs/2$) divided by the number of windows (Nw) defined on the calculation of the bivariable map. The scheme representing the IESFOgram procedure is shown in Fig. 3 and the step-by-step details for its extraction are described as follows.

Step 1: In the first step, the bi-variable map is extracted from the signal. The estimators of the $CSC(\alpha, f)$ can be based on the Averaged Cyclic Periodogram, the Cyclic Modulation Spectrum or any other numerical method [16] to extract the CSC bi-variable map previously described in Eq. 3. The CSC can also be in its normalized version $CSCoh(\alpha, f)$, and its cyclic variable α and spectral variable f can be represented in units of either frequency or orders of shaft speed. The user can define on its own discretion which method to use in order to obtain the bi-variable map $CSC(\alpha, f)$. The reader is forwarded to the references [19, 18], suggested as providers of the numerical implementation of the CSC in the Order-Frequency domain, and to the reference [15] to the Frequency-Frequency domain CSC, which if applied to the order tracked signal as a function of angle results in the Order-Order domain CSC.

Step 2: The next step consists in dividing the map along the spectral axis f according to the 1/3-binary tree that is also applied to the Fast Kurtogram [8]. Each tree is defined by a series with a decreasing bandwidth bw and incremental steps of center frequency cf which define the upper and the lower limit, f_1 and f_2 respectively, described in the integration of Eq. 5. Each band is then integrated

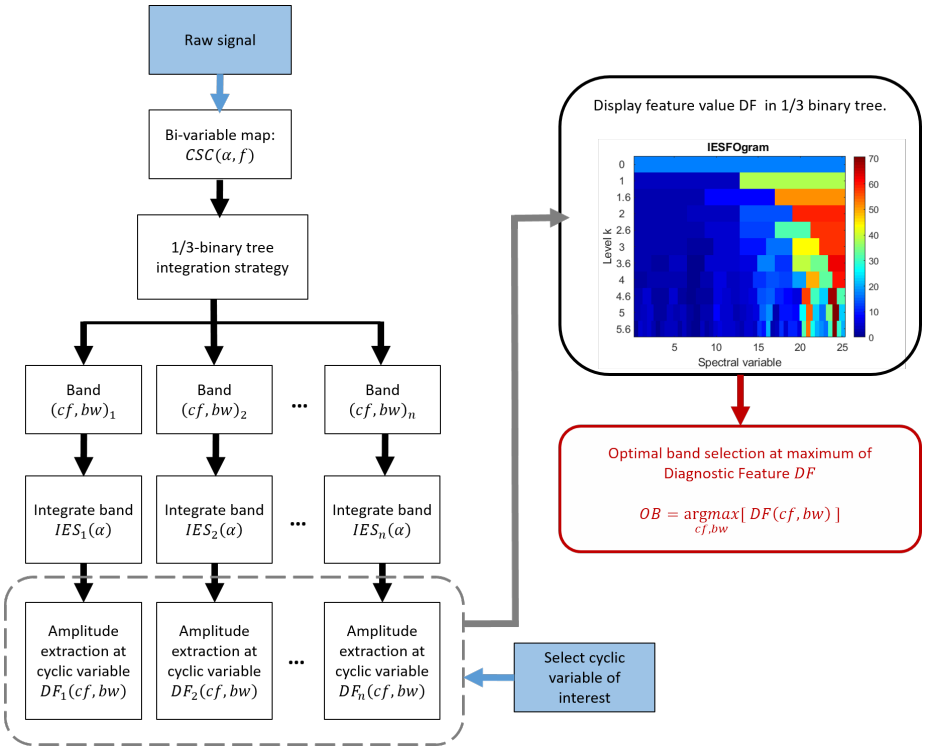

Figure 3: Schematic description of the IESFOgram procedure.

and results in a demodulated spectrum $IES_{cf,bw}(\alpha)$.

Step 3: From each processed $IES_{cf,bw}(\alpha)$, one Diagnostic Feature $DF(cf, bw)$ is extracted. This feature is based on the cyclic fault frequency/order of interest. Therefore, to calculate this feature, as well as the IESFOgram, this cyclic component needs to be loaded into the method as input. The feature $DF(n)$ is defined as the sum of the N-harmonics of the characteristic fault frequency/order α_{fault} normalized by the noise level estimated in a bandwidth $2 \times f_b$, as described in Eq. 8.

$$DF(cf, bw) = \sum_{k=1}^{N} \frac{IES_{cf,bw}(k \times \alpha_{fault})}{\frac{1}{2f_b}\left[\int_{kf_{fault}-f_b}^{kf_{fault}+f_b} IES_{cf,bw}(\alpha)d\alpha - IES_{cf,bw}(k \times alpha_{fault})\right]} \tag{8}$$

where α_{fault} is the characteristic frequency of interest (e.g. BPFO, BPFI, BSF, etc.), and f_b is the frequency band around the harmonics considered to be

the background noise. The normalization procedure is important to be taken into account. This is due to some bands having high peak values of noise, and the direct absolute value at the fault frequencies can be higher than at the optimal band. Normalizing with the background noise level at the peaks solves this problem, making high values of the DF to correspond to bands where the frequency peaks of interest are present. The authors found that a good background noise range f_b is 1/3 of the shaft frequency that modulates the bearing signal of interest. This value avoids capturing the sidebands around the α_{fault} and is simultaneously wide enough to provide a proper noise level. The maximum level of the 1/3 binary level defines the precision of the band, and high levels increase exponentially the computational cost for the IESFOgram. The authors found that a level between 5 and 7 for the computation of the 1/3 binary provides a good convergence for the optimal band.

Step 4: The objective of this step is to find the optimal band for integration of the bi-variable. To quantify the presence of a cyclic component in each band, the library of features $DF(cf, bw)$ is used. The higher the value of DF, the higher the presence of the component of interest. Thus, the optimal band OB is identified as the argument which maximizes $DF(cf, bw)$, as described in Eq. 9.

$$OB = \arg\max_{cf,bw}[\ DF(cf, bw)\ ] \tag{9}$$

The colormap presentation of the values of DF as a function of (cf, bw) in a 1/3-binary tree is the IESFOgram, and its maximum value corresponds to the selected optimal band for integration.

Step 5: The final step is the integration of the bi-variable map along the spectral axis on the optimal band OB selected by the IESFOgram. This step can be considered not being part of the IESFOgram procedure, but as the extraction of the IES with a high Signal-to-Noise Ratio (SNR) for diagnostic purposes.

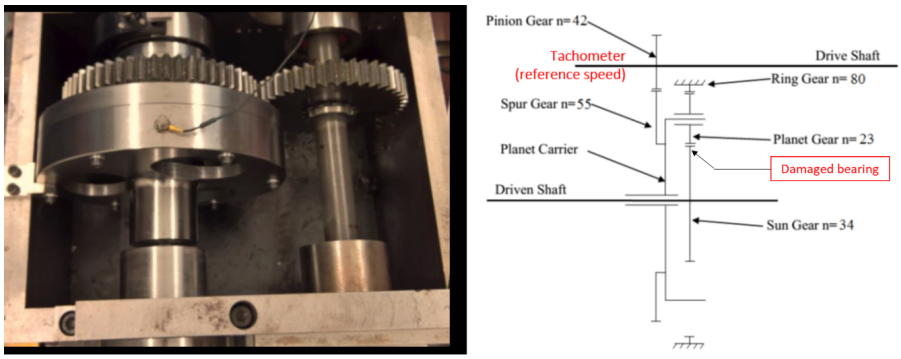

Figure 4: Test rig (left) inside view, (right) schematic representation.

4. Experimental application and results

In order to test and validate the proposed methodologies, vibration data have been captured from two separate test setups and divided into 3 case studies. One dataset corresponds to one laboratory planetary gearbox with one damaged bearing, and bearing diagnostics is studied under constant speed operating conditions in Case 1, and under varying speed conditions in Case 2. In Case 3 the vibration signals correspond to a dataset acquired from a aircraft engine gearbox with two damaged bearings under varying speed operating conditions.

4.1. Case 1- Planetary gearbox under constant speed conditions

In a first comparison, the case under constant speed conditions of 5.4 Hz of the input shaft speed is first studied. The vibration data have been captured on the UNSW planetary gear test rig, which consists of one parallel and one planetary gear stage as presented in Fig. 4.

The ring is fixed, while the output is the sun gear. The carrier is the input meshing with the parallel spur gear stage of the motor drive shaft. The teeth number of each gear is 80, 34 and 23 for the ring, sun and planet gears respectively. The planet gears rotate with a ratio of 2.66 times the drive shaft. The damaged bearing is a radial cylindrical roller bearing (IKO RNAF 162812) and is mounted on one of the planets. The damaged bearing has a fault on the outer race with a width of 1.6 mm, while its roller diameter is 3.0 mm. Thus

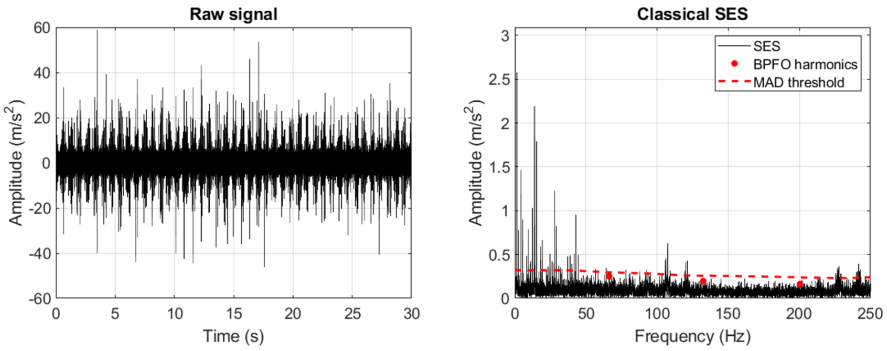

Figure 5: (left) Vibration signal, (right) SES.

the expected Ball Pass Order of the Outer Race fault (BPOO) is 12.3 orders of the drive shaft. For this case, with a constant input shaft speed of 5.4 Hz, the Ball Pass Frequency of the Outer race (BPFO) is 66.4 Hz.

In order to capture the vibration signal, one external accelerometer was mounted on the gearbox over the planet gears. The signals were acquired with
264 a sampling frequency of 150 kHz and synchronised by a National Instrument PXI data acquisition system. The signal was acquired for a duration of 30 seconds, and it can be seen in Fig. 5 alongside with its classical SES.

Classical demodulation by applying the Hilbert transform to the signal exhibits the gear meshing frequencies and the shaft speeds. However, it fails to exhibit the characteristic frequencies of the bearing fault, e.g. the harmonics of the BPFO. To define if the extracted amplitude value on the spectrum of the cyclic component are statistically relevant, a threshold is also calculated, and visualized on this spectrum, as well as on all other spectra presented in this paper. The threshold is the same as the one applied by Kaas *et. al.* [25] for detecting statistically relevant peaks in the spectra, based on 3 times the moving Median Absolute Deviation (MAD) of its spectra, defined as described in Eq.10.

$$MAD = 1.4826 \times m[\ |x - m(x)|\ ] \tag{10}$$

where $m(x)$ is the median of signal x. The window defined on all spectra corresponds to the total number of samples of each corresponding spectrum

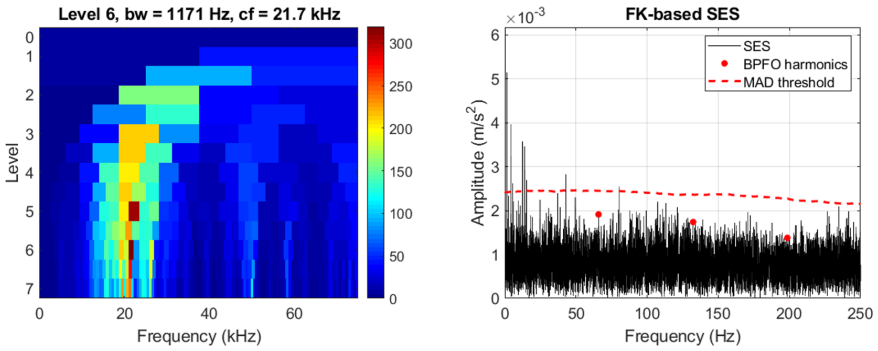

Figure 6: (left) Fast Kurtogram, (right) Filtered SES.

divided by 2^7. The threshold was suggested as a robust method for outlier detection in probabilistic studies in the psychology field because it is not as sensitive to outliers as the standard deviation [26]. Therefore, all values above the threshold are considered to be statistically relevant for detection of the frequency.

Applying the Fast Kurtogram and filtering on its selected band before the demodulation of the signal also does not result in the detection of fault frequencies. The Fast Kurtogram applied to the signal as well as the resulting SES based on its selected band is shown in Fig. 6.

The band with the maximum Spectral Kurtosis value does not result in the optimal band for filtering, and thus the FK-based SES does not exhibit statistically valid peak values at the BPFO. The same lack of diagnosis results from the Autogram-based SES, where the harmonics of the BPFO are not detected, as shown in Fig. 7.

The proposed IESFOgram is applied next to the CSCoh in the Frequency-Frequency domain, and both the IESFOgram and the IES from the integration on the band of frequencies selected by the IESFOgram can be seen in Fig. 8.

The IESFOgram shows a good performance in detecting the optimal band of frequencies in the CSCoh that contains the carrier of the BPFO harmonics. As such, the integration on this band results in a demodulated spectrum in the frequency domain, whose BPFO harmonics are well above the MAD threshold

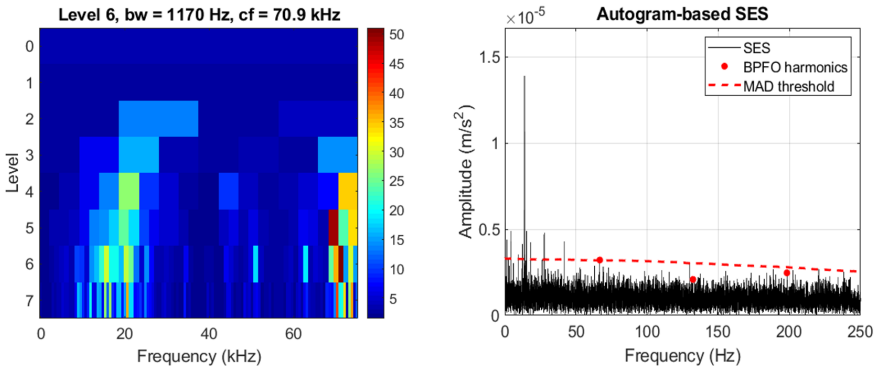

Figure 7: (left) Autogram, (right) Filtered SES.

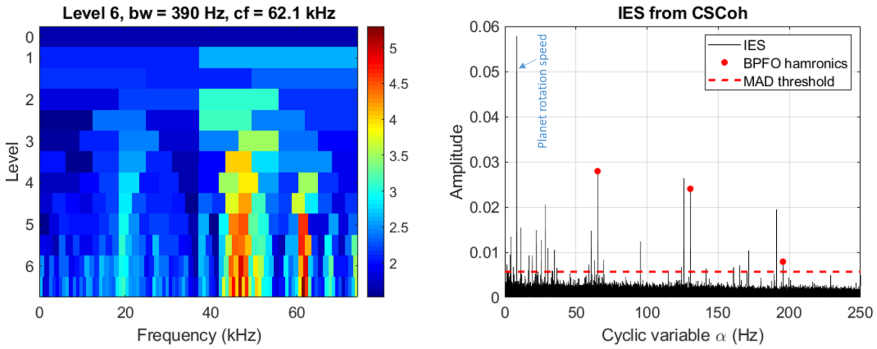

Figure 8: (left) IESFOgram, (right) IES from CSCoh.

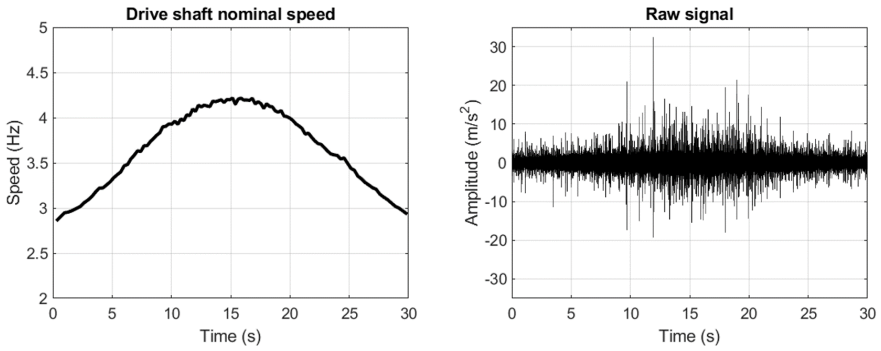

Figure 9: (left) Speed profile of the input shaft, (right) Vibration signal.

and the other components, present on the signal, are reduced. Additionally, the sidebands of the planet shaft speed of 2.66 orders that modulate the BPFO in planet bearing structures can also be detected in the spectrum. The detection of bearing damage is dependent on the quality of the measurements and its sensors. The accelerometers here acquire the signals at a high sampling frequency, which allows the IESFOgram to detect the carrier bands of frequency excited by the bearing damage, at 46 kHz and 62 kHz. In case the signals were at 50 kHz, observability of frequencies above the Nyquist would be lost, and detection of the BPFO harmonics would become unfeasible. As such, this method allows a confident diagnosis of the outer race damage on the planet bearing.

4.2. Case 2 - Planetary gearbox under varying speed conditions

In this case, the dataset from the same UNSW setup is studied, but the case is extended to operations under varying speed and therefore a case with a speed variation between 2.8 Hz and 4.2 Hz is tested. Due to the fact that the tachometer measures the speed of the drive shaft, all characteristic orders of the mechanism are calculated and referenced in relation to the drive shaft speed. The speed profile of the input shaft and the acquired vibration signal are shown in Fig. 9.

Under varying speed conditions, the bi-variable map needs to be either in the Order-Order domain or in the Order-Frequency domain. Starting with

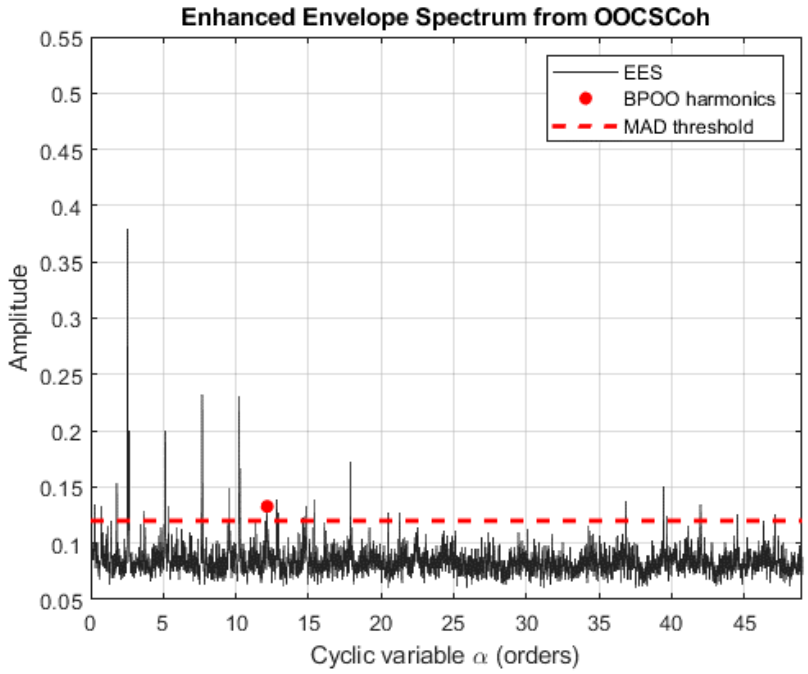

Figure 10: EES from OOCSCoh.

the Order-Order domain, the OOCSCoh is first calculated on the signal and the integration of its full available frequency band (from 0 Hz up to Nyquist frequency) is then realised. The resulting Enhanced Envelope Spectrum from the OOCSCoh is shown in Fig. 10.

The first BPOO harmonic can be detected already with this method, which gives an advantage when compared against the Fast Kurtogram and the Autogram based SES. However only the first harmonic is detected, and its amplitude is rather close to the threshold. Following this analysis, the IESFOgram is extracted based on the BPOO of 12.3 orders. The IESFOgram and the band selected by the diagnostic tool allows the clear identification of the BPOO after its integration on the Order-Order domain CSCoh. Both the resulting IESFOgram and the IES with the harmonics of the BPOO above the threshold are presented in Fig. 11.

When compared to the EES, the IES shows a higher performance in detecting

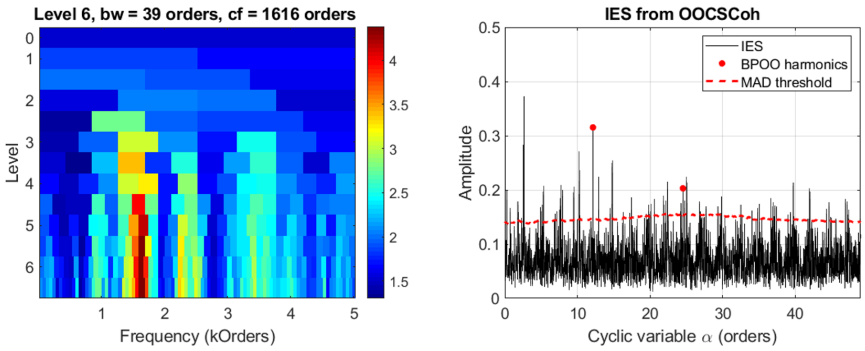

Figure 11: (left) IESFOgram, (right) IES from OOCSCoh.

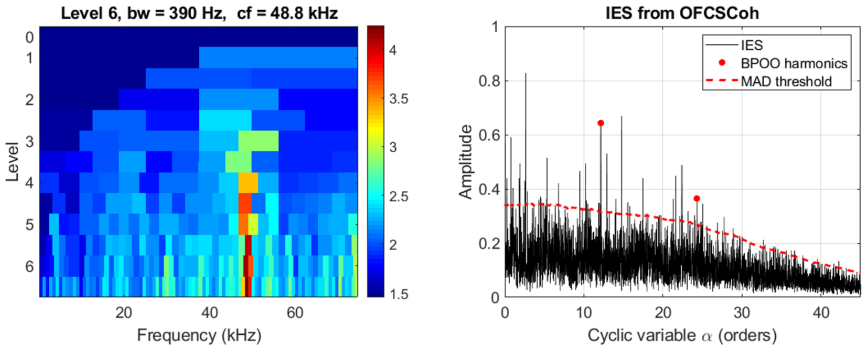

Figure 12: (left) Speed profile of the input shaft, (right) Vibration signal.

the presence of the outer race damage in the signal with its extraction of 2 harmonics above the threshold, and reduced presence of other components of the signal. The methodology is further applied on the CSCoh in the Order-Frequency domain. The IESFOgram is prepared and the extracted IES based on the selected integrated band is presented in Fig. 12. The first two harmonics of the BPOO can be identified in the spectrum above the threshold, allowing the clear detection and diagnosis of the outer race damage on the outer race of the planet bearing.

4.3. Case 3 - Planetary gearbox under varying speed conditions

The vibration signal from the Safran engine gearbox is analysed in this last case. The signal corresponds to 100 seconds at a sampling frequency of $fs = 50$

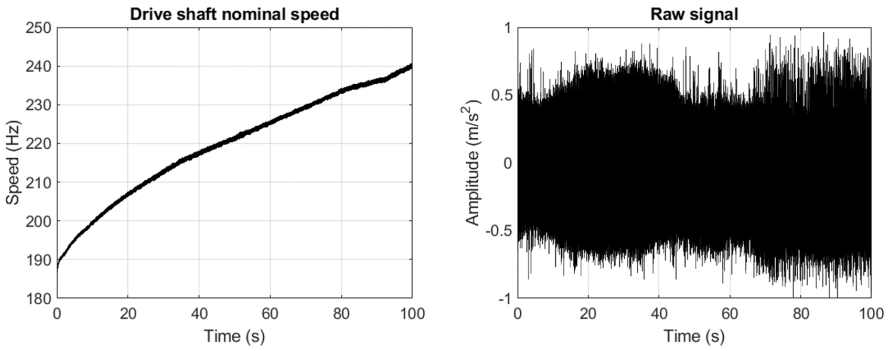

Figure 13: (left) IESFOgram, (right) IES from OFCSCoh.

kHz, under a run-up from 180 Hz to 210 Hz of the shaft rotation speed, as shown in Fig. 13. The vibration dataset was provided by Safran and corresponds to the Safran contest which took place during the Conference Surveillance. It was acquired under a lower sampling frequency than the one of the first two cases. The engine has two main shafts and an accessory gearbox. The kinematics of the gearbox are described in Fig. 14.

On the gearbox there are two damaged bearings: one on the radial drive shaft L1 and one on the shaft L5. The ball bearing on L1 is damaged on the outer race with a heavy scratch of 0.3 mm of depth and 1 mm of width. The roller bearing on shaft L5 is also damaged on the outer race but spalled on a wide area with a depth of 0.1 mm. The speed reference is obtained from the tachometer mounted on shaft L4, with a resolution of 44 pulses per revolution. The vibration signals came from two accelerometers. One accelerometer is mounted near the shaft L1 and the second one is mounted in the vicinity of shaft L5. The fault order for the ball bearing outer race damage on shaft L1 is 4.066 orders of the shaft L1 and the fault order for the roller bearing outer race damage is 7.759 orders of the shaft L5.

The vibration signal from the accelerometer near the L1 shaft was concluded to have issues on its acquisition leading to the lack of source signature of the fault bearings in the vibration signal. As such, only the signal acquired from the accelerometer near L5 is analysed in this paper, and the evidence of the

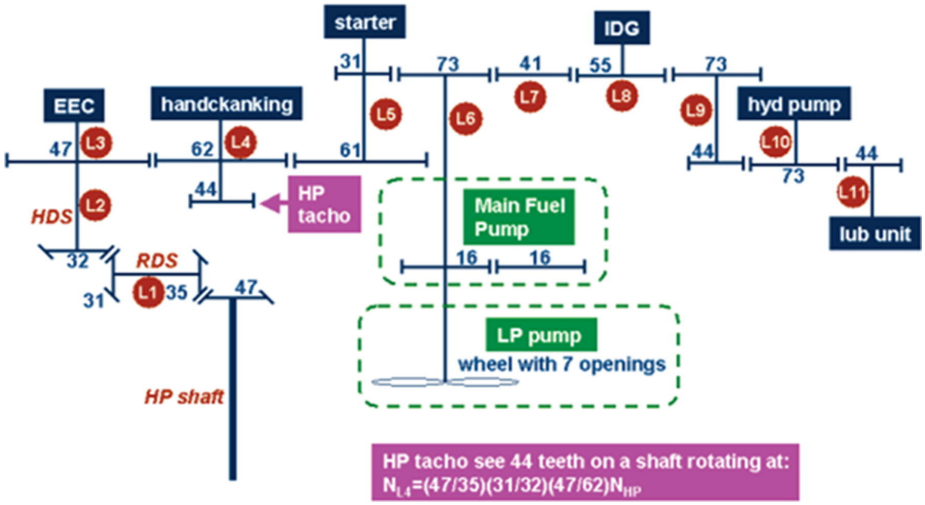

Figure 14: Safran gearbox schematic.

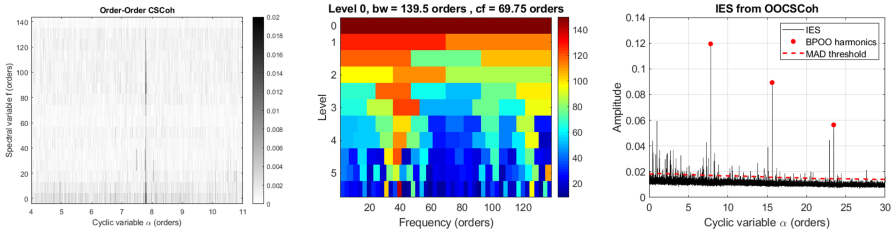

Figure 15: (left) Order-Order bi variable map zoomed around the BPOO, (middle) IESFOgram, (right) IES from the OOCSCoh.

presence of the outer-race fault of the bearing supporting shaft L5 is diagnosed.

The OOCSCoh is then estimated from the angular re-sampled signal. Next, the IESFOgram is extracted based on this bi-variable map. Afterwards, the IES based on the OOCSCoh is estimated based on the integration of the optimal band defined by the IESFOgram, as presented in Fig. 15

The method seems to select an optimal band that maximizes the first 3 harmonics of the BPOO. Upon closer analysis of the OOCSCoh, it is noticed that the BPOO is excited across several bands over the spectral axis. The diagnosis of the damage through the analysis of the map usually requires some level of expertise but on the other hand, the OOIES presents clearly the harmonics of

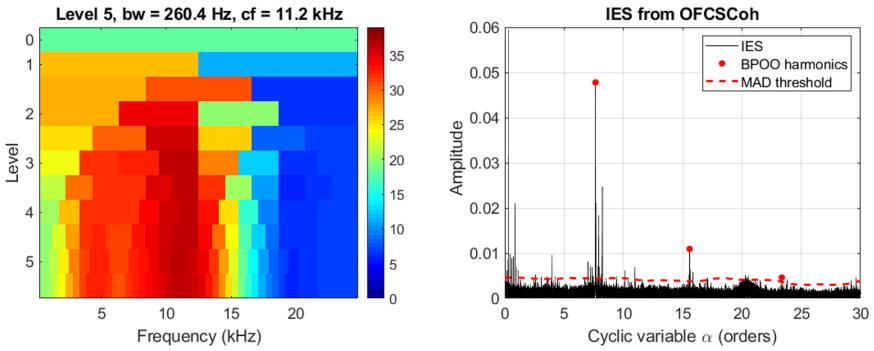

Figure 16: Safran gearbox schematic.

the damage on the spectrum, allowing a confident diagnosis.

The Order-Frequency CSCoh based methodology is then studied, and shows a similar result when compared to its Order-Order version, as the integration is realised over all the spectral content. However the bi-variable map shows the damage-related CS content to be more centralized on the middle range of frequencies of the spectral axis and the gears and shaft harmonics are reduced in the spectrum. This is most likely due to the nature of the OF-CSC theory, where the carrier information is kept as a function of time and thus not smearing the time-dependent carrier frequencies over the spectral axis.

When IESFOgram is applied on the OFCSCoh, the previous statement can be confirmed due to the selection of a narrow band, in the lower frequency spectrum, as the optimal band. The IESFogram and the resulting OFIES can be seen in Fig. 16.

This dataset also provides a good example on the complexity of the analysis for bi-variable maps. While the detection of the bearing damage cannot be extracted in a straightforward manner from the analysis of the bi-variable maps, the analysis of the resulting demodulated spectra provides a clear detection of the fault order.

5. Conclusion

A new method is proposed in this paper to find proper carrier frequency bands for bearing diagnostics based on the cyclo-non-stationary theory and bi-variable maps of three domains. At first, the Cyclic Spectral Coherence (CSCoh) bi-variable function on the Frequency-Frequency domain is extracted on cases under constant operating speed conditions. The bi-variable map shows good performance in revealing the hidden cyclic modulations generated by bearing damage. A Diagnostic Feature (DF) based on the bearing characteristic frequency is extracted on a series of bands along the spectral axis. The DF values are color-mapped in a 1/3-binary tree, named Improved Envelope Spectrum via Feature Optimization-gram (IESFOgram). Its maximum value corresponds to the optimal band, and its integration on the bi-variable map results in the Improved Envelope Spectrum (IES) with robust diagnosis performance.vThe procedure can be extended to cases under varying speed conditions. The speed profile needs to be known, with the objective of obtaining the bi-variable maps which provide a good representation of the signal, in either the Order-Order domain or the Order-Frequency domain. The advantage of the IESFOgram as a band selection tool is indeed that it can be applied in any of the three domains of the bi-variable maps. This means the methodology can be applied to either constant or varying speed conditions.vThe method has been tested on two datasets: one planetary gearbox dataset with a damaged planet bearing and one aircraft engine gearbox dataset with a damaged bearing. The IESFOgram has been compared with the Fast Kurtogram-based and the Autogram-based demodulation methods. The results demonstrate that the IESFOgram achieves higher performance, allowing to effectively detect the bearing damage, when compared to the other methods under constant speed conditions. The IESFOgram is further validated on the two datasets under varying speed conditions and it is concluded that it is a robust methodology for general bearing diagnostics.

Acknowledgment

The authors would like to thank Ali Moshrefzadeh and Alessandro Fasana for sharing the Autogram publicly. K. Gryllias gratefully acknowledges the Research Fund KU Leuven.

References

[1] S. Sheng, Wind turbine gearbox vibration condition monitoring benchmarking datasets, NREL/TP-5000-54530.

[2] F. P. G. Mrquez, A. M. Tobias, J. M. P. Prez, M. Papaelias, Condition monitoring of wind turbines: Techniques and methods, Renewable Energy 46 (2012) 169 – 178.

[3] J. Antoni, J. Griffaton, H. Andr, L. D. Avendao-Valencia, F. Bonnardot, O. Cardona-Morales, G. Castellanos-Dominguez, A. P. Daga, Q. Leclre, C. M. Vicua, D. Q. Acua, A. P. Ompusunggu, E. F. Sierra-Alonso, Feedback on the surveillance 8 challenge: Vibration-based diagnosis of a safran aircraft engine, Mechanical Systems and Signal Processing 97 (2017) 112 – 144, special Issue on Surveillance.

[4] F. Elasha, M. Greaves, D. Mba, Bearing signal separation of commercial helicopter main gearbox, Procedia CIRP 59 (2017) 111 – 115.

[5] L. Zhou, F. Duan, M. Corsar, F. Elasha, D. Mba, A study on helicopter main gearbox planetary bearing fault diagnosis, Applied Acoustics 147 (2019) 4 – 14, special Issue on Design and Modelling of Mechanical Systems conference CMSM2017.

[6] R. Randall, J. Antoni, Rolling element bearing diagnostics - a tutorial, Mechanical Systems and Signal Processing 25 (2011) 485–520.

[7] M. Feldman, Hilbert transform applications in mechanical vibration, John Wiley and Sons, 2011.

[8] J. Antoni, Fast computation of the kurtogram for the detection of transient faults, Mechanical Systems and Signal Processing 21 (1) (2007) 108 – 124.

[9] N. Sawalhi, R. B. Randall, The application of spectral kurtosis to bearing diagnostics, in: Proceedings of Acoustics 2004, Academic Press, 2004, pp. 393–398.

[10] A. Moshrefzadeh, A. Fasana, The autogram: An effective approach for selecting the optimal demodulation band in rolling element bearings diagnosis, Mechanical Systems and Signal Processing 105 (2018) 294 – 318.

[11] W. Smith, Z. Fan, Z. Peng, H. Li, R. Randall, Optimised spectral kurtosis for bearing diagnostics under electromagnetic interference, Mechanical Systems and Signal Processing 75 (2016) 371–394.

[12] P. W. Tse, D. Wang, The sparsogram: A new and effective method for extracting bearing fault features, in: 2011 Prognostics and System Health Managment Confernece, 2011, pp. 1–6.

[13] J. Antoni, The infogram: Entropic evidence of the signature of repetitive transients, Mechanical Systems and Signal Processing 74 (2016) 73 – 94, special Issue in Honor of Professor Simon Braun.

[14] R. Randall, J. Antoni, S. Chobsaard, The relationship between spectral correlation and envelope analysis in the diagnostics of bearing faults and other cyclostationary machine signals, Mechanical Systems and Signal Processing 15 (5) (2001) 945 – 962.

[15] J. Antoni, G. Xin, N. Hamzaoui, Fast computation of the spectral correlation, Mechanical Systems and Signal Processing 92 (2017) 248 – 277.

[16] P. Borghesani, J. Antoni, A faster algorithm for the calculation of the fast spectral correlation, Mechanical Systems and Signal Processing 111 (2018) 113 – 118.

[17] J. Antoni, Cyclic spectral analysis in practice, Mechanical Systems and Signal Processing 21 (2) (2007) 597 – 630.

[18] D. Abboud, J. Antoni, Order-frequency analysis of machine signals, Mechanical Systems and Signal Processing 87 (2017) 229 – 258.

[19] D. Abboud, S. Baudin, J. Antoni, D. Rmond, M. Eltabach, O. Sauvage, The spectral analysis of cyclo-non-stationary signals, Mechanical Systems and Signal Processing 75 (Supplement C) (2016) 280 – 300.

[20] R. Zimroz, W. Bartelamus, Gearbox condition estimation using cyclo-stationary properties of vibration signal, Key Engineering Material 413-414 (2009) 471 – 478.

[21] J. Wodecki, A. Michalak, R. Zimroz, T. Barszcz, A. Wylomanska, Impulsive source separation using combination of nonnegativematrix factorization of bi-frequency map, spatial denoising andmonte carlo simulation, Mechanical Systems and Signal Processing 127 (2019) 89 – 101.

[22] Y. Guo, T.-W. Liu, J. Na, R.-F. Fung, Envelope order tracking for fault detection in rolling element bearings, Journal of Sound and Vibration 331 (25) (2012) 5644 – 5654.

[23] J. Antoni, F. Bonnardot, A. Raad, M. E. Badaoui, Cyclostationary modelling of rotating machine vibration signals, Mechanical Systems and Signal Processing 18 (6) (2004) 1285 – 1314.

[24] G. D'Elia, M. Cocconcelli, E. Mucchi, An algorithm for the simulation of faulted bearings in non-stationary conditions, Meccanica 53 (4-5) (2018) 1147–116.

[25] S. Kass, A. Raad, J. Antoni, Self-running fault diagnosis method for rolling element bearing, Mechanism, Machine, Robotics and Mechatronics Sciences. Mechanisms and Machine Science 58 (2019) 127 – 140.

[26] C. Leys, O. Klein, P. Bernard, L. Licata, Detecting outliers: Do not use standard deviation around the mean, use absolute deviation around the median, Journal of Experimental Socal Psychology 49 (2013) 764–766.